Silylene Does React with Carbon Monoxide: Some Gas-Phase Kinetic and Theoretical Studies

Rosa Becerra

Instituto de Quimica-Fisica "Rocasolano", CSIC, C/Serrano 119, 28006 Madrid, Spain

J. Pat Cannady

Dow Corning Corporation, P.O. Box 995, Mail 128, Midland, Michigan 48686-0995

Robin Walsh*

Department of Chemistry, University of Reading, Whiteknights, P.O. Box 224, Reading RG6 6AD, U.K.

Received: November 20, 2000

Time-resolved studies of the reaction of silylene, SiH_2, with CO have been carried out over the pressure range 10−500 Torr (with SF_6 as bath gas) at four temperatures in the range 299−477 K, using laser flash photolysis to generate and monitor SiH_2. The second-order rate constants obtained were pressure dependent, indicating that the reaction is a third-body assisted association process close to its third-order limit. The second-order rate constants at a pressure of 100 Torr gave the following Arrhenius parameters: $\log(A/\mathrm{cm^3\ molecule^{-1}\ s^{-1}}) = -13.92 \pm 0.23$, $E_a = -13.02 \pm 1.62$ kJ mol^{-1}, where the uncertainties are single standard deviations. Ab initio calculations at the G2 level indicated formation of silaketene, H_2SiCO, as the initial product. RRKM theoretical calculations, employing a variational transition state based on the ab initio surface, fitted the kinetic data very well with a dissociation enthalpy, $H_D°(H_2Si{-}CO) = 89$ kJ mol^{-1}, in very good agreement with ab initio calculation. These studies show unequivocally that SiH_2 does react rapidly with CO and that an earlier gas-phase investigation was carried out under conditions unfavorable for the observation of reaction.

Introduction

Silylene, SiH_2, is known to react rapidly and efficiently with many chemical species.[1,2] Examples of its reactions include Si−H bond insertions, C=C and C≡C π-bond additions, and reactions with lone pair donors.[3] Many of these reactions occur at close to the collision rate.[1,2] It therefore appears somewhat surprising that direct, time-resolved kinetic studies by Chu et al.[4] of the reaction of SiH_2 with CO give an upper limit for the reaction rate constant of only 10^{-13} cm^3 molecule^{-1} s^{-1} (in the gas phase in 5 Torr of He buffer gas). This corresponds to a collision efficiency of less than 10^{-3}, and contrasts with the reaction of $^1CH_2 + CO$, which is at least 400 times faster.[5] The stimulus for the present reinvestigation of this reaction was the recent report by Maier et al.[6] of the IR spectrum of silaketene, H_2SiCO (the probable product of $SiH_2 + CO$), in a frozen Ar matrix at 12 K. The study was supported by quantum chemical calculations[6] which suggest that H_2SiCO is slightly more stable than previously thought ($H_2Si{-}CO$ binding energy of 90−100 as opposed to 67 kJ mol^{-1} [7]). The story is somewhat paralleled by the situation with respect to the potential reaction between dimethylsilylene, $SiMe_2$, and CO, where no gas-phase reaction could be found in our laboratory,[8] while matrix isolation studies[9,10] strongly point to formation of Me_2SiCO.

One of the possible causes for the lack of reaction in the earlier kinetic studies[4] could have been the low pressure employed (5 Torr), allied with the inefficiency of helium as a collision partner. Thus, the reaction might well initially form vibrationally excited silaketene as shown in reaction 1, but which may rapidly redissociate via breaking of its weak bond unless collisionally stabilized. In other words this is potentially a classic example of an association reaction requiring a third body.

$$H_2Si + CO \rightleftarrows H_2SiCO^* \xrightarrow{M} H_2SiCO \qquad (1)$$

Thus, to try to resolve this apparent anomaly, we have reinvestigated the kinetics of this reaction in the gas phase at much higher pressures and with SF_6, a known efficient collision partner, as bath gas. At the same time we decided to carry out our own ab initio calculations to assist with RRKM modeling of the reaction rate pressure dependence. A preliminary account of this work has appeared.[11]

Experimental Section

Equipment, Chemicals, and Method. The apparatus and equipment for these studies have been described in detail previously.[12,13] Only essential and brief details are therefore included here. SiH_2 was produced by the 193 nm flash photolysis of phenylsilane, $PhSiH_3$, using a Coherent Compex 100 exciplex laser. Photolysis pulses were fired into a variable-temperature quartz reaction vessel with demountable windows, at right angles to its main axis. SiH_2 concentrations were monitored in real time by means of a Coherent 699-21 single-mode dye laser pumped by an Innova 90-5 argon ion laser and operating with rhodamine 6G. The monitoring laser beam was multipassed between 32 and 48 times along the vessel axis, through the reaction zone, to give an effective path length of

10.1021/jp004259f CCC: $20.00
Published on Web 02/07/2001

up to 1.8 m. A portion of the monitoring beam was split off before entering the vessel for reference purposes. The monitoring laser was tuned to 17 259.50 cm^{-1}, corresponding to a known strong vibration−rotation transition[12,14] in the SiH_2 $A(^1B_1) \leftarrow X(^1A_1)$ absorption band. Light signals were measured by a dual photodiode/differential amplifier combination, and signal decays were stored in a transient recorder (Datalab DL910) interfaced to a BBC microcomputer. This was used to average the decays of up to 10 photolysis laser shots (at a repetition rate of 1 or 2 Hz). The averaged decay traces were processed by fitting the data to an exponential form using a nonlinear least-squares package. This analysis provided the values for first-order rate coefficients, k_{obs}, for removal of SiH_2 in the presence of known partial pressures of substrate gas.

Gas mixtures for photolysis were made up, containing between 1.5 and 6.5 mTorr of $PhSiH_3$ and 0−20 Torr of CO together with inert diluent (SF_6) at total pressures between 10 and 500 Torr. Pressures were measured by capacitance manometers (MKS, Baratron).

All gases used in this work were thoroughly degassed prior to use. $PhSiH_3$ (99.9%) was obtained from Ventron-Alfa (Petrarch). Carbon monoxide, CO, (99.96%) was obtained from Argo International Ltd. Sulfur hexafluoride, SF_6 (no GC-detectable impurities), was from Cambrian Gases.

Ab Initio Calculations. The electronic structure calculations were performed with the Gaussian 94 software package.[15] All structures were determined by energy minimization at the MP2=Full/6-31G(d) level. Transition-state structures were characterized as first-order saddle points by calculation of the Hessian matrix. Stable structures, corresponding to energy minima, were identified by possessing no negative eigenvalues of the Hessian, while transition states were identified by having one and only one negative eigenvalue. The standard Gaussian-2 (G2) compound method[16] was employed to determine final energies for all structures, both for energy minima and transition states. The identities of the transition-state structures were verified by calculation of intrinsic reaction coordinates[17] (IRCs) at the MP2=Full/6-31G(d) level. Reaction barriers were calculated as differences in G2 enthalpies at 298.15 K.

Results

Kinetics. Preliminary experiments quickly established that at ambient temperatures SiH_2 does react with CO when pressures of ca. 10 Torr are used. It was also found at the outset of the investigation that SiH_2 decay constants, k_{obs}, depended not only on CO pressures but also on total pressures. Other preliminary checks showed that, for a given reaction mixture, k_{obs} values were not dependent on the exciplex laser energy (50−80 mJ/pulse, routine variation) or number of photolysis shots (up to 10 shots). The constancy of k_{obs} (5 shot averages) showed no effective depletion of reactants. The sensitivity of detection of SiH_2 was very high but decreased with increasing temperature and pressure. Therefore, slightly higher quantities of $PhSiH_3$ precursor were required under the latter conditions. For the purposes of rate constant measurement at a given temperature, $PhSiH_3$ pressures were kept fixed. At room temperature, 299 K, a series of experiments was undertaken to investigate the dependence of k_{obs} on CO pressure. Each set was carried out at a fixed total pressure using SF_6 diluent. Partial pressures of CO were varied between 0 and 10 Torr, at nine different total pressures between 10 and 500 Torr. A pressure of 500 Torr is the highest practical one which can be achieved with our existing equipment. The results of five of these sets of experiments are shown in Figure 1, which demonstrates the linear dependence of k_{obs} with [CO] expected for second-order kinetics. The second-order rate constants, obtained by least-squares fitting to these plots, are collected in Table 1. The error limits are single standard deviations. It is clear that the rate constants increase with increasing pressure.

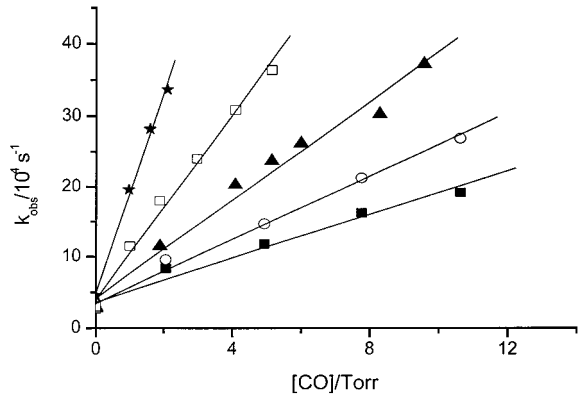

Figure 1. Some second-order plots of the dependence of k_{obs} on carbon monoxide pressure at different overall pressures (Torr) (SF_6) at 299 K: ■, 20; ○, 30; ▲, 50; □, 100; ★, 200.

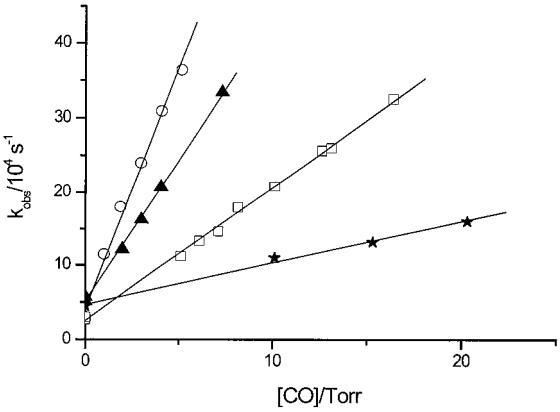

Figure 2. Some second-order plots of the dependence of k_{obs} on carbon monoxide pressure in SF_6 (100 Torr) at different temperatures (K): ○, 299; ▲, 337; □, 397; ★, 477.

TABLE 1: Experimental Second-Order Rate Constants ($k/10^{-12}$ cm^3 $molecule^{-1}$ s^{-1}) for SiH_2 + CO at Different Temperatures and Pressures

P/Torr	299 K	337 K	397 K	477 K
10	0.276 ± 0.007			
20	0.499 ± 0.028	0.291 ± 0.09		
30	0.713 ± 0.023	0.425 ± 0.012	0.256 ± 0.011	
50	1.08 ± 0.06	0.633 ± 0.020	0.381 ± 0.013	
100	2.03 ± 0.08	1.33 ± 0.02	0.741 ± 0.011	0.278 ± 0.008
150	3.49 ± 0.23	1.97 ± 0.08	1.18 ± 0.02	0.446 ± 0.011
200	4.41 ± 0.16	2.88 ± 0.04	1.54 ± 0.05	0.677 ± 0.013
400	7.91 ± 0.09	5.13 ± 0.03	2.61 ± 0.07	1.23 ± 0.03
500	9.63 ± 0.47	6.54 ± 0.03	3.00 ± 0.06	1.37 ± 0.05

These experiments were then repeated at three other higher temperatures of 337, 397, and 477 K, to explore the temperature dependence of the reaction. As can be seen from the results below, the rates decrease with increasing temperature, and thus higher pressures of CO were needed at higher temperatures. In practice up to 20 Torr of CO was used.

The upper limit of temperature was determined by the need to get a reasonable total pressure range with a predominance of SF_6 diluent. The results of a selection of these experiments at a fixed total pressure of 100 Torr are shown in Figure 2, which demonstrates the linear dependence of k_{obs} with [CO] expected for second-order kinetics, at each temperature. The second-order

TABLE 2: Arrhenius Parameters as a Function of Pressure[a]

P/Torr	log(*A*/cm^3 molecule^{-1} s^{-1})	E_a/kJ mol^{-1}	*P*/Torr	log(*A*/cm^3 molecule^{-1} s^{-1})	E_a/kJ mol^{-1}
100	-13.92 ± 0.23	-13.02 ± 1.62	400	-13.19 ± 0.19	-12.16 ± 1.35
150	-13.76 ± 0.20	-13.29 ± 1.35	500	-13.33 ± 0.16	-13.46 ± 1.09
200	-13.49 ± 0.15	-12.43 ± 1.04			

[a] Pressures below 100 Torr not included because of insufficient data.

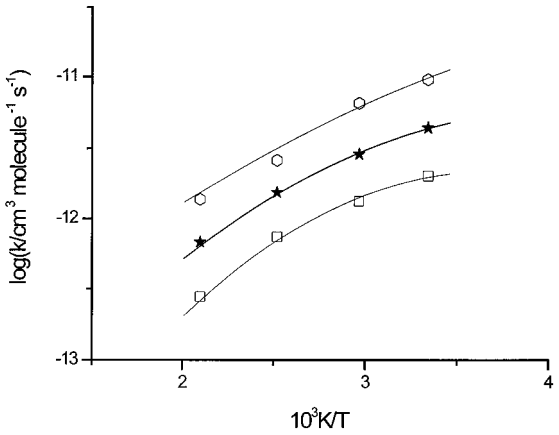

Figure 3. Arrhenius plots of the second-order rate constants for SiH_2 + CO at different total pressures (Torr): ⬡, 500; ★, 200; □, 100.

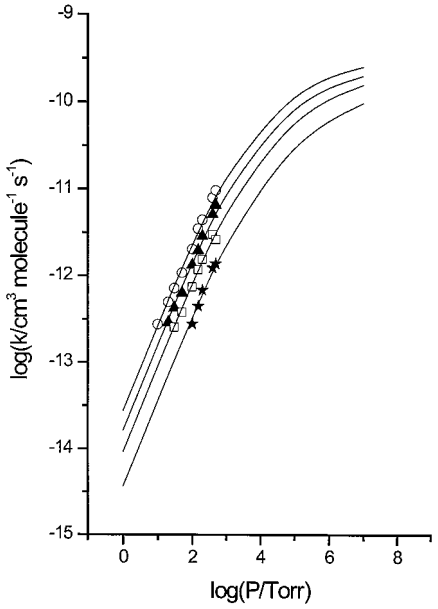

Figure 4. Pressure dependence of the second-order rate constants for SiH_2 + CO in the presence of SF_6 at different temperatures (K): ○, 299; ▲, 337; □, 397; ★, 477. Curves are RRKM theory fits (see the text).

rate constants at the other temperatures and pressures are also shown in Table 1. It is clear that the rate constants decrease with increasing temperature. Arrhenius plots of these were made at each pressure. Figure 3 shows three such plots at 100, 200, and 500 Torr. The others are not shown to avoid congesting the graph. There is a hint of curvature in these plots as the pressure decreases. However, the data within reasonable error limits can be made to fit a linear form. The resulting Arrhenius parameters are shown in Table 2. Clearly the activation energies are not significantly pressure dependent within the range investigated.

The combined results of the pressure and temperature dependence experiments are shown in Figure 4, where the pressure dependencies of the rate constants at each temperature

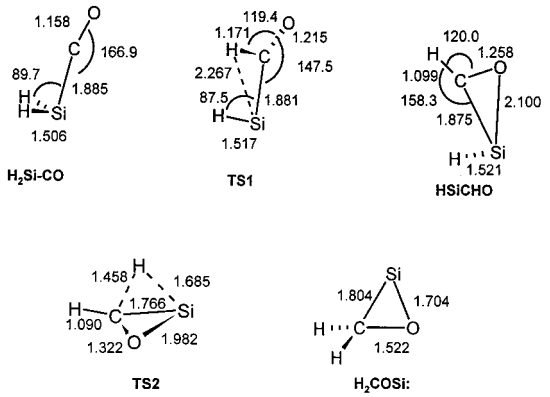

Figure 5. Ab initio MP2=Full/6-31G(d) calculated geometries of local minimum structures and transition states on the SiH_2 + CO energy surface. Selected distances are given in angstroms and angles in degrees.

are presented in a log−log plot for convenience. It can be seen that these pressure dependence plots are almost linear. Least-squares fitting to these plots gave the following gradients: 0.92 ± 0.02 (299 K), 0.98 ± 0.02 (337 K), 0.90 ± 0.03 (397 K), and 1.00 ± 0.07 (477 K). These results are characteristic of a third-body assisted association reaction and indicate that the reaction is close to its third-order kinetic limit under the conditions of study. By extrapolation to low pressures, we estimate the rate constants for the third-order region, *k*/cm^6 molecule^{-2} s^{-1}, to be $(9.0 \pm 2.0) \times 10^{-31}$ (at 299 K), $(5.4 \pm 1.3) \times 10^{-31}$ (at 337 K), $(4.0 \pm 1.0) \times 10^{-31}$ (at 397 K), and $(1.6 \pm 0.4) \times 10^{-31}$ (at 477 K). To assist with the theoretical interpretation of these results, we have carried out RRKM calculations preceded by ab initio calculations, described in the following sections.

Ab Initio Calculations. These were undertaken to lay the basis for RRKM modeling. Thus, one of the chief points of interest was how the energy of interaction of the silylene and carbon monoxide varied during the reaction approach. As a preliminary to such a calculation, a number of possible species on the $CSiH_2O$ surface were investigated in some detail at the G2 level of theory. Apart from the reactants, SiH_2 + CO, and probable product, H_2SiCO, silaketene, three other energy minima and two transition states were found. The minima corresponded to formylsilylene, HSiCHO, siloxiranylidene, c-CH_2SiO, and the O-bonded complex $H_2Si\cdots OC$. The transition state linking H_2SiCO and HSiCHO is called TS1, and that linking HSiCHO and c-CH_2SiO is called TS2. The structures of these species are shown in Figure 5, and their enthalpy values are listed in Table 3, as well as being represented on the potential energy (enthalpy) surface in Figure 6. Among the notable features of the surface are (i) the relatively strongly bound silaketene species, (ii) the relatively small, although positive barrier to H-migration (TS1) for H_2SiCO to HSiCHO, (iii) the higher barrier for cyclization with H-transfer (TS2) for HSiCHO to c-CH_2SiO, although the latter species is the lowest energy species on the surface, and (iv) the very weakly bound, less favorable O-bonded complex.

No barrier seems to exist for formation of silaketene from the reactants. Because of this, potential energy scans were

TABLE 3: Ab Initio (G2) Enthalpies for CH_2SiO Species of Interest in the Reaction of Silylene with Carbon Monoxide

molecular species	enthalpy/hartrees	rel energy/kJ mol^{-1}	molecular species	enthalpy/hartrees	rel energy/kJ mol^{-1}
$SiH_2 + CO$	403.338 090 0	0	HSiCHO	403.338 566 0	0
$H_2SiC{\equiv}O$	403.372 938 0	−92	TS2	403.312 842 1	+67
TS1	403.332 336 5	+17	c-CH_2SiO	403.378 358 0	−105

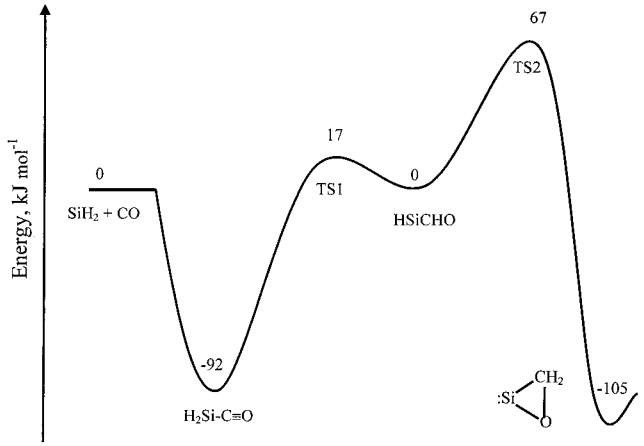

Figure 6. Potential energy (enthalpy) surface for the reaction of SiH_2 + CO. All enthalpies were calculated at the ab initio G2 level.

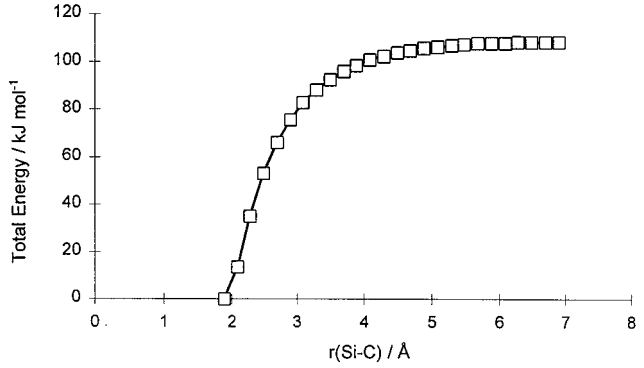

Figure 7. Variation of the total energy (MP2=Full/6-31G(d)) with Si−C separation during the dissociation of silaketene.

performed by freezing the Si−C bond separation at various values and optimizing the remaining coordinates at the HF/6-31G(d), B3LYP/6-31G(d), and MP2=Full/6-31G(d) levels. Frequency calculations were carried out on a selected set of these structures at the HF/6-31G(d) level. In this manner a picture was built up of the variation of all of these quantities as a function of Si−C separation. Figure 7 shows the energy variation at the MP2=Full/6-31G(d) level.

As far as geometry is concerned, the outcome of the calculations was that the silaketene structure is maintained as the Si−C separation increases, with the other bond lengths hardly changing and the SiH_2 moiety maintaining its perpendicular configuration relative to the almost linear Si−C−O bond axis. Of the vibrational wavenumbers, only the transitional modes, viz., the SiH_2 group rocking modes and the Si−C−O bends, show significant changes (drops in values) as the Si−C bond increases.

RRKM Calculations. If there are no competing side reactions, the pressure dependence of an association reaction corresponds exactly to that of the reverse unimolecular dissociation process. The ab initio calculations suggest no competing processes, and the only ongoing process for the initially formed silaketene has a positive energy barrier, which suggests that it will not be competitive. We have therefore carried out RRKM calculations[18] of the pressure dependence of the unimolecular decomposition of silaketene, i.e.

TABLE 4: Estimated Thermodynamic and Kinetic Quantities for Silaketene Decomposition (Reactions −1 and +1)

T/K	ΔS/J K^{-1} mol^{-1} [a]	T/K	$\log(A_{-1}/s^{-1})$ [b]
300	132.6	299	15.88
400	131.8	337	15.82
500	130.5	397	15.72
		477	15.59

[a] From ab initio calculations. [b] Calculated using eq 2.

$$H_2SiCO \rightleftarrows SiH_2 + CO \qquad (-1, +1)$$

In principle all the information required for these calculations is available from the ab initio calculation. However, the biggest uncertainty is the binding energy of SiH_2 with CO, in other words the dissociation energy of $H_2Si{-}CO$, which represents the critical energy, E_o, and is taken as a variable in these calculations. For the first stage in the construction of a transition-state structure for this reaction, we have estimated decomposition A factors using the equation

$$\Delta S^\circ = R \ln(A_{-1}/A_{+1}) \qquad (2)$$

The entropy values, ΔS°, are taken from the G2 ab initio calculation, which included the calculation of the individual thermodynamic properties of all species involved. These are shown in Table 4, together with the values of $\log A_{-1}$ calculated from eq 2 using an assumed value of $\log(A_1/cm^3\ molecule^{-1}\ s^{-1}) = -10.0$. This value was taken by analogy with that found for the similar reaction of $SiH_2 + C_2H_4$[19] and based on the assumption of a loose transition state, suggested by the experimental results obtained here of a fairly fast reaction. There is no published value for $S^\circ(H_2SiCO)$, but the magnitude of $\Delta S^\circ(-1,+1) = 132.6$ J K^{-1} mol^{-1} may be judged by comparison with the equivalent entropy change for $CH_2CO \rightleftarrows {}^1CH_2 + CO$ for which published data[20] give $\Delta S^\circ = 144$ J K^{-1} mol^{-1}. This is expected to be larger because of the tight allene-like structure of ketene, which releases more entropy upon dissociation than loose, weakly bound silaketene. It seems unlikely that $\Delta S^\circ(-1,+1)$ will be significantly in error. The biggest uncertainty will be associated with A_1, but this was varied within the reasonable limits of $10^{\pm 0.5}$, which should therefore correspond to the effective uncertainty range for the A_{-1} values of Table 4. A_{-1} values decline slightly with temperature as has been found in many SiH_2 reaction systems.[13,19,21,22]

The next stage in the calculations was to determine the structure and assign the vibrational wavenumbers to the molecule and its activated complex. In our preliminary calculation[11] we used an assignment based on the matrix IR spectrum of Maier et al.[6] for silaketene. Here, for consistency we have used the HF/6-31G(d) results for both the molecule and activated complex, with the 0.893 correction factor for calculated harmonic frequencies.[23] In this exercise the activated complex structure was systematically varied by alteration of the Si−C separation until the resulting parameters (moments of inertia and vibrational wavenumbers) gave an entropy value which matched the entropy of activation and thereby the A factor *at each temperature*. This has the effect of building in variational

TABLE 5: Molecular and Transition-State Parameters for RRKM Calculations for Silaketene Decomposition

		complex			
	molecule	299 K	337 K	397 K	477 K
r(Si−C)/Å[a]	2.037	4.180	4.095	3.972	3.850
inertia ratio (I^+/I)		2.99	2.89	2.75	2.61
vib wavenumbers/cm^{-1}	2183	2186	2186	2188	2188
	1985	1981	1981	1980	1980
	1977	1971	1971	1970	1970
	947	1010	1010	1010	1010
	734	146	157	174	195
	729	114	122	135	152
	277[b]				
	246	49	52	57	62
	241	49	52	57	62
$Z_{LJ}/10^{-10}$ cm^3 molecule^{-1} s^{-1} [c]		4.56	4.63	4.74	4.88

[a] Si−C separation imposed on ab initio calculation. [b] Reaction coordinate. [c] Lennard-Jones collision number for H_2SiCO^* with SF_6.

character to the calculation. This is the first time we have been able to use ab initio calculations in this way to reduce some of the arbitrariness of transition-state assignment. However, it should be borne in mind that RRKM calculations are not particularly sensitive to these details provided the entropy of activation is matched.[18] The details of the calculations are given in Table 5. In these calculations we have assumed that rotational effects (angular momentum conservation problems) are approximately taken care of by the moment of inertia changes. We have treated the transitional modes as vibrations and not internal rotations, since the Si−C−O portion of the molecule is effectively linear and (as the ab initio calculation shows) the bending motion is effectively degenerate. There may be some uncertainty in the model here, but we believe it is unlikely to lead to serious errors. We have used a weak collisional (stepladder) model for collisional deactivation,[18] since there is considerable evidence against the strong collision assumption.[24] For most of our calculations we employed an average energy removal parameter, $\langle\Delta E\rangle_{down}$ of 12.0 kJ mol^{-1} (1000 cm^{-1}) as used previously in other similar reaction systems.[19,22] However, in some calculations we tried other values in the range 6−12 kJ mol^{-1}. There was some evidence (see below) in favor of a lower value for this parameter.

The critical energy, E_o, was treated as an adjustable parameter to not prejudge the ab initio calculations, the only source of information on the bond dissociation energy $D(H_2Si-CO)$. We showed in our preliminary calculation[11] that a value of E_o = 90 kJ mol^{-1} provides a reasonable fit to the data at 299 K. That was based on a transition-state model with a higher A factor ($10^{16.4}$ s^{-1}) than the one recommended here. With the slightly tighter transition state of Table 4, we have found the best fit corresponds to E_o = 77 kJ mol^{-1} (values of 84, 90, and 96 kJ mol^{-1} were also tried). The criterion for fitting the data in the reaction studied here is somewhat different from those of the systems investigated previously,[13,19,21,22] where curvature in the falloff region and extrapolation to the high-pressure limit could be used. In the present case, closeness to the second-order limit was the main criterion. This could be judged in two ways, as the incremental gradient in the log−log plots and as the degree of falloff at a particular pressure. Using the first of these criteria, the incremental gradient between 10 and 100 Torr had values of between 0.94 (at 299 K) and 0.96 (at 477 K), and using the second, the degree of falloff at 100 Torr had values of between $10^{2.0}$ (at 299 K) and $10^{2.5}$ (at 477 K). These incremental gradients are in good agreement with the measured gradients (see the Discussion), and the degrees of falloff imply high-pressure limiting rate constants (cm^3 molecule^{-1} s^{-1}) of between $10^{-9.6}$ and $10^{-10.0}$. For higher values of E_o (>77 kJ mol^{-1}) the incremental gradients were less (and lower than experiment). For lower values of E_o (<77 kJ mol^{-1}) the degree of falloff was greater to the point of being too great (where the implied high-pressure limit is greater than the collision number). The resulting curves are shown together with the data in Figure 4.

TABLE 6: Comparison of the Degree of Falloff, log(k/k^∞) at 100 Torr for Different Step Sizes[a,b]

T/K	log(k/k^∞)[a]	log(k/k^∞)[b]	T/K	log(k/k^∞)[a]	log(k/k^∞)[b]
299	−2.042	−2.189	397	−2.291	−2.535
337	−2.154	−2.341	477	−2.480	−2.786

[a] $\langle\Delta E\rangle_{down}$ = 12 kJ mol^{-1}. [b] $\langle\Delta E\rangle_{down}$ = 6 kJ mol^{-1}.

The only other things which could have affected the choice of E_o were the magnitude of A_{-1} and the size of $\langle\Delta E\rangle_{down}$. In testing for A_{-1}, we found that a change of a factor of $10^{\pm0.5}$ corresponded to a change of ±13 kJ mol^{-1} in E_o, in a compensating way (a higher A factor implies a higher E_o and vice versa). For $\langle\Delta E\rangle_{down}$ we found that a reduction from 12 to 6 kJ mol^{-1} made little difference in the low-pressure incremental gradient, but affected the degree of falloff more significantly. To illustrate this difference, the degrees of falloff (in log form) at 100 Torr are compared in Table 6. The data show that, for the weaker collisions, the degree of falloff increases more sharply with temperature. For $\langle\Delta E\rangle_{down}$ = 12 kJ mol^{-1}, this corresponds to an activation energy difference of E_a(100 Torr) − $E_a(\infty)$ = −6.6 ± 0.5 kJ mol^{-1}, whereas if $\langle\Delta E\rangle_{down}$ = 6 kJ mol^{-1}, this corresponds to E_a(100 Torr) − $E_a(\infty)$ = −9.1 ± 0.6 kJ mol^{-1}. Incidently the Arrhenius plots (not shown) of both sets of relative rate constants (k/k^∞) show the same kind of curvature (convex upward) as the Arrhenius plots of Figure 3.

Thus, the activation energy difference, E_a(100 Torr) − $E_a(\infty)$, may be used as a third criterion for assessing the data. We found that it is independent of the choice of E_o (within the range of values examined). To a good approximation, it therefore depends only on the collisional model. However, no comparison with experiment can be made without a knowledge of $E_a(\infty)$, and this can only be obtained by fitting the RRKM-generated falloff curves to experiment (since the high-pressure limit is inaccessible under experimental conditions). When this was done, as in Figure 4, for both the sets of calculations (with their different energy removal parameters) and the k^∞ values obtained were fitted to the Arrhenius equation, the Arrhenius parameters shown in Table 7 resulted. These values can then be combined with those for log(A(100 Torr)/$A(\infty)$) and E_a(100 Torr) − $E_a(\infty)$, and the Arrhenius parameters for P = 100 Torr are thus obtained. These are in good agreement with those of Table 2, which demonstrates the self-consistency of the procedure. What this exercise does reveal, however, is that the parameter combinations contributing to the low-pressure Arrhenius parameters are significantly different. For $\langle\Delta E\rangle_{down}$ = 12 kJ mol^{-1}, a more temperature-dependent high-pressure limiting rate constant with $E_a(\infty)$ = −5.6 kJ mol^{-1} is required than for $\langle\Delta E\rangle_{down}$ = 6 kJ mol^{-1} for which $E_a(\infty)$ = −3.0 kJ mol^{-1}. The uncertainty in the choice of $\langle\Delta E\rangle_{down}$ cannot be conclusively settled by this argument, but the differing high-pressure Arrhenius parameters may be considered and compared with values for other reactions, as in the Discussion.

Dissociation Enthalpy of Silaketene. This may be simply obtained from E_o. Correction for thermal energy at 298 K gives E_a for reaction −1, $E_a(-1)$ = 83.5 kJ mol^{-1}. Then the enthalpy change, $\Delta H^o(-1,+1)$ = 89.0 kJ mol^{-1}, is obtained via

TABLE 7: Comparison of RRKM-Derived, Low-Pressure (100 Torr) Activation Energies at Different Step Sizes

$\langle\Delta E\rangle_{down} = 12$ kJ mol^{-1} (1000 cm^{-1})	
$\log(A^\infty/\text{cm}^3\ \text{molecule}^{-1}\ \text{s}^{-1}) = -10.56$	E_a/kJ mol^{-1} = −5.58
$\log(A(100\ \text{Torr})/A^\infty) = -3.19$	$(E_a(100\ \text{Torr}) - E_a)$/kJ mol^{-1} = −6.64
$\log(A(100\ \text{Torr})/\text{cm}^3\ \text{molecule}^{-1}\ \text{s}^{-1} = -13.75$	$E_a(100\ \text{Torr})$ /kJ mol^{-1} = −12.20
$\langle\Delta E\rangle_{down} = 6$ kJ mol^{-1} (500 cm^{-1})	
$\log(A^\infty/\text{cm}^3\ \text{molecule}^{-1}\ \text{s}^{-1}) = -9.99$	E_a/kJ mol^{-1} = −3.03
$\log(A(100\ \text{Torr})/A^\infty) = -3.76$	$(E_a(100\ \text{Torr}) - E_a)$/kJ mol^{-1} = −9.08
$\log(A(100\ \text{Torr})/\text{cm}^3\ \text{molecule}^{-1}\ \text{s}^{-1} = -13.75$	$E_a(100\ \text{Torr})$/kJ mol^{-1} = −12.11

$\Delta H^o(-1,+1) = E_a(-1) - E_a(+1) + RT$. This value assumes the weaker collisional model ($\langle\Delta E\rangle_{down} = 6$ kJ mol^{-1}) is operative. With the stronger collisional model, $\Delta H^o(-1,+1)$ becomes 91.6 kJ mol^{-1}. Other uncertainties in the value of $\Delta H°(-1,+1)$ are hard to assess but derive almost entirely from uncertainties in the RRKM modeling. Because the model is constrained by a number of considerations as described above, we doubt the total uncertainty exceeds ±10 kJ mol^{-1}.

Discussion

General Comments and Comparisons. The point of this work has been to demonstrate that silylene does indeed react with CO. This has been achieved and puts right the apparent anomaly that, whereas the reaction product, silaketene, has been detected in a matrix[6] and shown to be stable by quantum chemical calculations,[6,7] no reaction between SiH_2 and CO could be found in the gas phase.[4] The results obtained here have demonstrated that the gas-phase reaction is a third-body assisted association reaction near its third-order kinetic limit, and that without sufficient pressure of a reasonably strong collider gas, the rate will be significantly slowed. Under the conditions of the previous investigation, Chu et al.[4] obtained a rate constant upper limit of 1.0×10^{-13} cm^3 molecule^{-1} s^{-1} for reaction in 5 Torr of helium at room temperature. From our results (Table 1) by extrapolation we can see that in 5 Torr of SF_6 we would expect a rate constant of 1.4×10^{-13} cm^3 molecule^{-1} s^{-1}. Since the collision efficiency of SF_6 is 3−4 times greater than that of He in a number of thermal reactions,[24,25] we should expect the rate constant in 5 Torr of He to be ca. 4×10^{-14} cm^3 molecule^{-1} s^{-1}, consistent with the earlier findings.[4]

To get close to the high-pressure limit in this system, the calculations suggest that pressures of ca. 10^7 Torr are required, which is clearly unachievable with our existing equipment. Nevertheless, the RRKM modeling, discussed in more detail below, indicates that to be consistent with our results requires a limiting high rate constant, k_1^∞, of ca. $(2.5-3.4) \times 10^{-10}$ cm^3 molecule^{-1} s^{-1} at ambient temperatures. We have calculated the Lennard-Jones collision number for reaction 1, using standard procedures and sources described in an earlier paper,[26] and obtained a value of 3.8×10^{-10} cm^3 molecule^{-1} s^{-1}. Thus, the reaction has a collision efficiency of over 60%, which may even be 100%. Thus, the true association step (reaction 1) of SiH_2 with CO, far from being inefficient, may in fact occur on every collision! In this respect the reaction of SiH_2 with CO now clearly resembles those of its reactions with C_2H_2,[27] C_2H_4,[19] C_3H_6,[21] *i*-C_4H_8,[21] and Me_2CO.[22] It is also likely that it shares the high *A* factor and small negative activation energy characteristic of these reactions.

RRKM Calculations, Thermochemistry, and the Potential Energy Surface. The main objective of the calculations was to verify that a reasonable energy surface, and in particular a reasonable Si−C binding energy in silaketene, was consistent with the kinetic findings of a nearly third-order reaction. The RRKM calculations have shown this to be the case. A loose transition state was required because of the fast reaction rate. Uncertainties in the "looseness" of the transition state were largely eliminated through the requirement to fit the observed third-order kinetics with a reaction which did not exceed the collision rate (at high pressures). The structure and vibrational wavenumbers of the transition state were obtained from the ab initio calculations along the reaction coordinate, which readily accommodated its variational character. The critical energy, E_o = 77 kJ mol^{-1}, was obtained by systematic variation to obtain a best fit to the data, at all temperatures. The remaining uncertainty of the weak collisional energy removal parameter, $\langle\Delta E\rangle_{down}$, was shown not to make any substantial difference in the calculated outcome, although the evidence (from the low-pressure activation energy) favors a value for this parameter closer to 6 kJ mol^{-1}, rather than the 12 kJ mol^{-1} which seems to fit the modeling of similar reaction systems. It may be that, because the energized species in this system has only five atoms and the excitation energies are not high in this reaction, the average removed per collision is smaller.

The value for $\Delta H°(-1,+1) = H_D°(H_2Si{-}CO) = 89.0(\pm10)$ kJ mol^{-1}, obtained by combining the experimental results with the RRKM modeling, is in strikingly good agreement with the G2 calculation reported here of 92 kJ mol^{-1}, but ca. 16 kJ mol^{-1} higher than earlier calculations of Hamilton and Schaefer[7] (who report $\Delta H(0\ \text{K}) = 64-67$ kJ mol^{-1}). On the other hand, it is slightly lower than the 90−110 kJ mol^{-1} range reported by Maier et al.[6] (who quote ΔE without specifying the temperature) from MP2/6-31G** and B3LYP/6-31G** calculations. These differences in theory could maybe be reduced by further refinements, but within the experimental uncertainty are almost in agreement.

The fact that the reaction kinetics fit an association mechanism well is evidence that there is no available alternate reaction pathway for rearrangement or decomposition of silaketene other than by reversion to SiH_2 and CO. The calculated potential energy surface of Figure 6 is consistent with this since it shows a positive barrier of 17 kJ mol^{-1} to formation of formylsilylene, HSiCHO. This process would be further restricted by the requirement of a tight transition state for the H-migration process involved. The next potential stage on the surface is the ring closure of HSiCHO with H-migration to form siloxiranylidene, c-CH_2SiO, which has a barrier of 67 kJ mol^{-1} and is even more unlikely even though c-CH_2SiO is the lowest point of the surface. The energy surface obtained by us is very similar to the one calculated by Maier et al.[6] (at the B3LYP/6-31G** level) except that in their calculation c-CH_2SiO was marginally higher in energy than H_2SiCO (by 2.5 kJ mol^{-1}). Maier et al.[6] were able to identify experimentally both H_2SiCO and c-CH_2SiO by their IR spectra in an Ar matrix at 12 K. In their experiments the species were prepared by co-condensation of Si atoms with CH_2O, followed by vis/UV irradiation of the matrix.

We have not explored the potential energy surface further, because the structures and energetics obtained by us are in broad agreement with the existing and more extensive calculations of Maier et al.[6] The portion of the surface reinvestigated by us offers convincing theoretical support for the kinetic findings.

Acknowledgment. We thank the Direccion General de Investigacion Cientifica y Tecnica (DGICYT) for support to R.B. under Project PB98-0537-CO2-01. We also thank Monty Frey for helpful discussion.

References and Notes

(1) Jasinski, J. M.; Becerra, R.; Walsh, R. *Chem. Rev.* **1995**, *95*, 1203.

(2) Becerra, R.; Walsh, R. Kinetics & mechanisms of silylene reactions: A prototype for gas-phase acid/base chemistry. In *Research in Chemical Kinetics*; Compton, R. G., Hancock, G., Eds.; Elsevier: Amsterdam, 1995; Vol. 3, p 263.

(3) Gaspar, P. P.; West, R. Silylenes. In *The Chemistry of Organic Silicon Compounds*; Rappoport, Z., Apeloig, Y., Eds.; Wiley: Chichester, 1998; Vol. 2, Chapter 43, p 2463.

(4) Chu, J. H.; Beach, D. B.; Estes, R. D.; Jasinski, J. M. *Chem. Phys. Lett.* **1988**, *143*, 135.

(5) Langford, A. O.; Petek, H.; Moore, C. B. *J. Chem. Phys.* **1983**, *78*, 6650.

(6) Maier, G.; Reisenauer, H.-P.; Egenolf, H. *Organometallics* **1999**, *18*, 2155.

(7) Hamilton, T. P.; Schaefer, H. F., III. *J. Chem. Phys.* **1989**, *90*, 1031.

(8) Baggott, J. E.; Blitz, M. A.; Frey, H. M.; Lightfoot, P. D.; Walsh, R. *Int. J. Chem. Kinet.* **1992**, *24*, 127.

(9) Arrington, C. A.; Petty, J. T.; Payne, S. E.; Haskins, W. C. K. *J. Am. Chem. Soc.* **1988**, *110*, 6240.

(10) Pearsall, M.-A.; West, R. *J. Am. Chem. Soc.* **1988**, *110*, 7229.

(11) Becerra, R.; Walsh, R. *J Am. Chem. Soc.* **2000**, *122*, 3246.

(12) Baggott, J. E.; Frey, H. M.; King, K. D.; Lightfoot, P. D.; Walsh, R.; Watts, I. M. *J. Phys. Chem.* **1988**, *92*, 4025.

(13) Becerra, R.; Frey, H. M.; Mason, B. P.; Walsh, R.: Gordon, M. S. *J. Chem. Soc., Faraday Trans.* **1995**, *91*, 2723.

(14) Jasinski, J. M.; Chu, J. O. *J. Chem. Phys.* **1988**, *88*, 1678.

(15) Frisch, M. J.; Trucks, G. W.; Schlegel, H. B.; Gill, P. M. W.; Johnson, B. G.; Robb, M. A.; Cheeseman, J. R.; Keith, T.; Petersson, G. A.; Montgomery, J. A.; Raghavachari, K.; Al-Laham, M. A.; Zakrzewski, V. G.; Ortiz, J. V.; Foresman, J. B.; Cioslowski, J.; Stefanov, B. B.; Nanayakkara, A.; Challacombe, M.; Peng, C. Y.; Ayala, P. Y.; Chen, W.; Wong, M. W.; Andres, J. L.; Replogle, E. S.; Gomperts, R.; Martin, R. L.; Fox, D. J.; Binkley, J. S.; Defrees, D. J.; Baker, J.; Stewart, J. P.; Head-Gordon, M.; Gonzales, C.; Pople, J. A. *Gaussian 94*, Revision E.2; Gaussian Inc.: Pittsburgh, 1995.

(16) Curtiss, L. A.; Raghavachari, K.; Trucks, G. W.; Pople, J. A. *J. Chem. Phys.* **1991**, *94*, 7221.

(17) Gonzales, C.; Schlegel, H. B. *J. Chem. Phys.* **1989**, *90*, 2154.

(18) Holbrook, K. A.; Pilling, M. J.; Robertson, S. H. *Unimolecular Reactions*, 2nd ed.; Wiley: Chichester, 1996.

(19) Al-Rubaiey N.; Walsh, R. *J. Phys. Chem.* **1994**, *98*, 5303.

(20) Benson, S. W. *Thermochemical Kinetics*, 2nd ed.; Wiley: New York, 1976.

(21) Al-Rubaiey N.; Carpenter, I. W.; Walsh, R.; Becerra, R.; Gordon, M. S. *J. Phys. Chem. A* **1998**, *102*, 8564.

(22) Becerra, R.; Cannady, J. P.; Walsh, R. *J. Phys. Chem. A* **1999**, *103*, 4457.

(23) Pople, J. A.; Scott, A. P.; Wong, M. W.; Radom, L. *Isr. J. Chem.* **1993**, *33*, 345.

(24) Hippler, H.; Troe, J. In *Advances in Gas-Phase Photochemistry and Kinetics*; Ashfold, M. N. R., Baggott, J. E., Eds.; Royal Society of Chemistry: London, 1989; Vol. 2, Chapter 5, p 209.

(25) Quack, M.; Troe, J. In *Gas Kinetics and Energy Transfer*; Ashmore, P. G., Donavan, R. J., Eds.; Specialist Periodical Reports; The Chemical Society: London, 1977; Vol. 2, Chapter 5, p 175.

(26) Becerra, R.; Boganov, S.; Walsh, R. *J. Chem. Soc., Faraday Trans.* **1998**, *94*, 3569.

(27) Becerra, R.; Walsh, R. *Int. J. Chem. Kinet.* **1994**, *26*, 45.